

# Discovery of Human HMG-Coa Reductase Inhibitors using Structure-Based Pharmacophore Modeling Combined with Molecular Dynamics Simulation Methodologies

Minky Son, Chanin Park, Ayoung Baek, Shalini John, and Keun Woo Lee

**Abstract**—3-hydroxy-3-methylglutaryl coenzyme A reductase (HMGR) catalyzes the conversion of HMG-CoA to mevalonate using NADPH and the enzyme is involved in rate-controlling step of mevalonate. Inhibition of HMGR is considered as effective way to lower cholesterol levels so it is drug target to treat hypercholesterolemia, major risk factor of cardiovascular disease. To discover novel HMGR inhibitor, we performed structure-based pharmacophore modeling combined with molecular dynamics (MD) simulation. Four HMGR inhibitors were used for MD simulation and representative structure of each simulation were selected by clustering analysis. Four structure-based pharmacophore models were generated using the representative structure. The generated models were validated used in virtual screening to find novel scaffolds for inhibiting HMGR. The screened compounds were filtered by applying drug-like properties and used in molecular docking. Finally, four hit compounds were obtained and these complexes were refined using energy minimization. These compounds might be potential leads to design novel HMGR inhibitor.

**Keywords**—Anti-hypercholesterolemia drug, HMGR inhibitor, Molecular dynamics simulation, Structure-based pharmacophore modeling.

## I. INTRODUCTION

THE 3 hydroxy-3-methylglutaryl coenzyme A reductase (HMGR) catalyzes the conversion of HMG-CoA to mevalonate using two molecules of NADPH as cofactor and the enzyme is involved in rate-controlling step of mevalonate pathway which is related with biosynthesis of cholesterol and other isoprenoids [1]-[2]. Structure of HMGR was represented in Fig. 1. Structurally, *human* HMGR monomer consists of three domains: (1) The small, helical amino-terminal N-domain

Minky Son is with the Division of Applied Life Science (BK21 program), Gyeongsang National University (GNU), 501 Jinju-daero, Gazwa-dong, Jinju 660-701, Republic of Korea (phone: +82-55-772-1360; fax: +82-55-772-1359; e-mail: minky@bio.gnu.ac.kr).

Chanin Park is with the Division of Applied Life Science (BK21 program), Gyeongsang National University (GNU), 501 Jinju-daero, Gazwa-dong, Jinju 660-701, Republic of Korea (e-mail: chip@bio.gnu.ac.kr).

Ayoung Baek is with the Division of Applied Life Science (BK21 program), Gyeongsang National University (GNU), 501 Jinju-daero, Gazwa-dong, Jinju 660-701, Republic of Korea (e-mail: abaek@bio.gnu.ac.kr).

Shalini John is with the Division of Applied Life Science, Gyeongsang National University (GNU), 501 Jinju-daero, Gazwa-dong, Jinju 660-701, Republic of Korea (e-mail: shalini@bio.gnu.ac.kr).

Keun Woo Lee is with the Division of Applied Life Science (BK21 program), Gyeongsang National University (GNU), 501 Jinju-daero, Gazwa-dong, Jinju 660-701, Republic of Korea (phone: +82-55-772-1360; fax: +82-55-772-1359; e-mail: kwlee@bio.gnu.ac.kr).

(2) The large, central L-domain that contains the dimerization motif ENVIG (3) The small, S-domain which is inserted into the L-domain and contains a NAD(P) binding motif DAMGMN [1]. Inhibition of HMGR is considered as effective way to lower cholesterol levels so it is drug target to treat hypercholesterolemia, major risk factor of cardiovascular disease. So far, several statins are well known as HMGR inhibitors and some of these drugs are used in treating patients with cardiovascular disease. Statins have HMG-like moiety and bind to the active site of HMGR instead of substrate [3]. However, several reports reveal that statins cause diverse side effects such as eczema, sensory disturbances, depression, and muscle weakness [4]-[7]. Therefore, there is a need for developing HMGR inhibitor design to have potent activity and fewer side effects. In this study, to discover novel HMGR inhibitor, we performed structure-based pharmacophore modeling combined with molecular dynamics simulation approach. Four inhibitors including two statins, named as rosuvastatin and simvastatin, were used for molecular dynamics (MD) simulation study and the representative structure of each simulation were selected by clustering analysis. Four structure-based pharmacophore models were generated using the representative structure of structures of each complex. The generated pharmacophore models were validated using data set and used in virtual screening process to find novel scaffolds for inhibiting HMGR protein. The screened compounds were then filtered by applying drug-like properties and used in molecular docking calculation. As a result, four hit compounds were obtained and these complexes were refined using energy minimization. These compounds with chemical modifications might be virtual leads for HMGR inhibitor design.

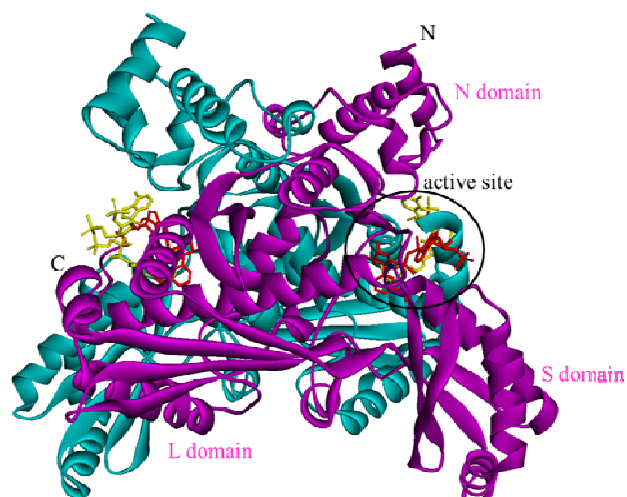


Fig. 1 Dimeric structure of human HMGR. Each monomer was represented magenta and cyan ribbon model, respectively and bound ligands in two identical active sites were displayed as red (NADP) and yellow (CoA) stick models

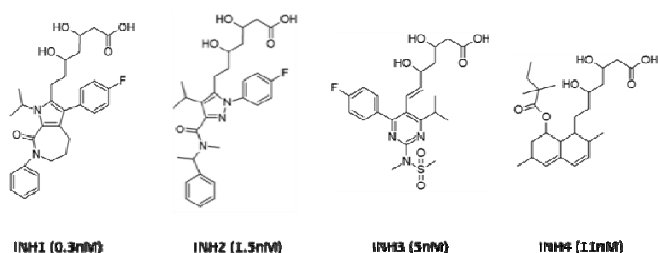


Fig. 2 Chemical structure of four HMGR inhibitors along with their IC<sub>50</sub> value

## II. METHODS

### A. Preparation of Systems

3D structures of human HMGR including ligand bound were available in Protein Data Bank. Among these structures, we selected complex structure with HMG, CoA, and NADP<sup>+</sup> (PDB code 1DQA). Using this structure, we built complex structures with four different HMGR inhibitors which were selected based on inhibitory activity and their scaffolds [3], [8]-[9]. We used dimeric form of the protein and all water molecules were removed.

### B. Molecular Dynamics Simulation

Including apo form, five systems were prepared for MD simulation study. All simulations were carried out using GROMACS 4.5.3 package with CHARMM27 force field [10]-[11]. While preparing, topology and force field parameters for inhibitors and cofactors were generated by SwissParam [12]. First of all, the protonation states of all the ionizable residues in protein were fixed to pH7 and hydrogen atoms were added. The structure was positioned in cubic water box with 10 Å from the protein surface and then solvated using TIP3P water molecules [13]-[14]. Some water molecules were replaced with Na counter-ions to neutralize the system. After that, the system was

subjected to energy minimization of 10000 steps using steepest descent algorithm. Next, position restrained MD was performed for 100 ps under NPT conditions at 300K to equilibrate the system and equilibrated system was used in 10 ns production runs. During the production runs, all bonds and the geometry of water molecules were restrained by LINCS [15]-[16] and SETTLE algorithm [17], respectively. The interaction energies like long-range electrostatic interaction and van der Waals were calculated using particle mesh Ewald (PME) algorithm [18]-[19] and cut-off of 14 Å. The pressure and temperature were maintained using a Parrinello-Rahman [20] barostat using Berendsen thermostat [21]. In case of calculation of fast Fourier transform, grid spacing with 1.2 Å was applied. To evade edge effects, the simulation was run under periodic boundary conditions. To obtain representative structure of each system, cluster analysis was performed using the trajectories from 4 ns to 10 ns. All other analyses containing, root mean square deviations (RMSD), potential energy, the number of intra and inter hydrogen bonds, and root mean square fluctuation (RMSF) were done through analysis tools implemented in GROMACS.

### C. Structure-Based Pharmacophore Model Generation

Structure-based pharmacophore models of four complexes were generated using their representative structure by Discovery Studio (DS) v3.1. Receptor-ligand pharmacophore generation protocol available in DS produces pharmacophoric features on the basis of interaction between the residues of protein and substrate. In the pharmacophore model generation, a sphere for the calculation was defined at the active site by Define and Edit Binding Sites tool in DS. Basic chemical properties such as hydrogen bond acceptor (HBA), hydrogen bond donor (HBD), hydrophobic (HYP), ring aromatic (RA), negative ionizable (NI) and positive ionizable (PI) were considered as pharmacophoric features and parameters were properly adjust to handle the flexibility of protein. As a result, total ten hypotheses were obtained and ranked by selectivity score. Top-scoring hypothesis was chosen as final pharmacophore model and it was comprised of vital pharmacophoric features necessary to inhibitory activity. Finally four pharmacophore models were obtained from four representative structures.

### D. Validation of Pharmacophore Model and Virtual Screening

Final pharmacophore model of each system was validated with data set consisting of 12 HMGR inhibitors, 361 aldose reductase inhibitors, and 89 glutathione reductase inhibitors. These inhibitors have inhibitory activity with IC<sub>50</sub> values and all inhibitors were used in energy minimization using DS. Ligand Pharmacophore Mapping protocol were used in the validation process and 12 HMGR inhibitors were used as active and the rest compounds of data set as inactive. To find novel scaffold which satisfy pharmacophoric features of each models, virtual screening process was performed using the validated pharmacophore models. In the stage, four data bases named as ASINEX, Chembridge, Maybridge, and NCI were employed.

The screened compounds from this stage were sorted to check their drug-likeness. Lipinski's rule of five [22] and ADMET (Absorption, Distribution, Metabolism, Excretion and Toxicity) [23] properties were calculated via DS. In the last stage, the compounds passing all criteria were selected for molecular docking calculation.

#### E. Molecular Docking and Energy Minimization

The compounds selected from virtual screening and drug-likeness properties calculation were subjected to molecular docking study using GOLD 5.0.1 (Genetic Optimization for Ligand Docking), from the Cambridge Crystallographic Data Centre, Cambridge, U.K [24]-[25]. In the docking for hit and reference compounds (HMGR inhibitors), the residues within 15 Å from the center of active site were defined as binding site for calculation. The value of GA runs was increased up to 50 for accuracy. Additionally, early termination option was used for efficiency so if any five poses were within the RMSD value of 1.5 Å, the calculation was quitted and moved on the next ligand. The resultant poses were then ranked according to GOLD fitness score. From the predicted binding conformation of hit compounds, we analyzed molecular interactions in the active site of HMGR. In case of the selected compounds from molecular docking, we calculated binding free energy using AutoDock 4.2. It predicts the interaction of ligands with biomacromolecular targets [26]-[27] and estimates the binding free energy upon bound conformations of flexible ligands based on Lamarckian genetic algorithm (LGA). To refine complex structures of final hit compounds, energy minimization was performed using GROMACS and all structural analyses of final hit compound were done with these structures.

### III. RESULTS

#### A. Construction of Protein-Inhibitor Complex

Total four HMGR inhibitors were chosen from literatures based on highly active and their scaffolds. Fig. 2 represents chemical structure of four inhibitors with their IC<sub>50</sub> values. All inhibitors have HMG-like moiety and potent inhibitory activity. INH1 and INH2 were pyrrole-based and pyrazole-based compounds. INH3 and INH4 were known for a member of statins, called rosuvastatin and simvastatin, respectively. In case of INH3 was structurally similar with other statins, but it differed in containing sulfur atom. INH4 was one of the approved statin drugs and widely used for lowering cholesterol and triglycerides in the blood. Four HMGR-inhibitor complexes were used in MD simulation study.

#### B. Molecular Dynamics Simulation of Five Complex

10 ns MD simulation study was performed using five complex (TABLE I) including apo form and inhibitor bound form to investigate structural changes and to consider structural flexibility when developing structure-based pharmacophore models. Prior to analysis, overall stability of system was checked using RMSD and potential energy calculations. As shown in Fig. 3, all simulations were stable during 10 ns with no abnormal conformational changes.

TABLE I  
FIVE COMPLEXES USED IN THIS STUDY

No	System	details
1	Apo	HMGR_NADPH
2	INH1	HMGR_NADPH_INH1
3	INH2	HMGR_NADPH_INH2
4	INH3	HMGR_NADPH_INH3
5	INH4	HMGR_NADPH_INH4

#### C. Comparison of Five Complex Using Representative Structure from Cluster Analysis

To compare each system, we obtained representative structure from 6000 structures after 4 ns using cluster analysis. In the cluster analysis, conformational families of each system were statistically classified as clusters according to the cut-off value and the value is 0.135 nm, 0.132 nm, 0.126 nm, 0.127 nm, and 0.134 nm in Apo, INH1, INH2, INH3, and INH4 complex, respectively. From the cluster analysis, the middle structure was selected as representative structure of each system. When apo form was superimposed with each inhibitor bound form, structural deviations were not much with the RMSD value of 1.05 Å (INH1-Apo), 1.2 Å (INH2-Apo), 1.09 Å (INH3-Apo), and 1.35 Å (INH4-Apo), respectively.

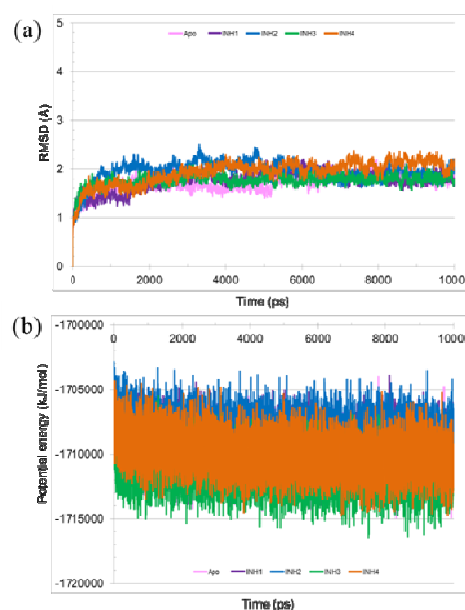


Fig. 3 RMSD and potential energy plots. (a) C<sub>α</sub> RMSD (b) potential energy during 10 ns MD simulations of all systems

#### D. Binding Mode of Four HMGR Inhibitors

Binding mode of four inhibitors was shown in Fig. 4. All inhibitors showed reasonable binding mode and formed hydrogen bond network with active site residues of HMGR. In case of HMGR in complex with INH1, the inhibitor formed hydrogen bonds with R590, S684, K691, S565, A751, K735, N755, and NADPH. Also, hydrophobic interactions were observed in INH1 binding; R590 formed cation- $\pi$  interaction with fluorophenyl group of INH1 and S865 formed  $\pi$ - $\sigma$  interaction with phenyl group of INH1. In case of HMGR-INH2 complex, the residues such as R590, D690, K691, E559, S565, K735, N755, and NADPH were participated in

hydrogen bond interactions with INH2. The  $\pi$ - $\pi$  interactions between INH2 and imidazole rings of aromatic residues like H866 and H869 were detected. In HMGR-INH3 complex, the residues R590, S684, D690, K691, S565, K735, N755, H869, and NADPH have involved in hydrogen bonds with INH3. In HMGR-INH4 complex, INH4 has formed hydrogen bonds with R590, S684, D690, E559, K735, H752, N755, S865, and NADPH. Unlike three other systems, hydrogen bond with S565 was not found in INH4 binding and this was mainly due to the strong hydrogen bonding with S865 which is located on the opposite side of S565.

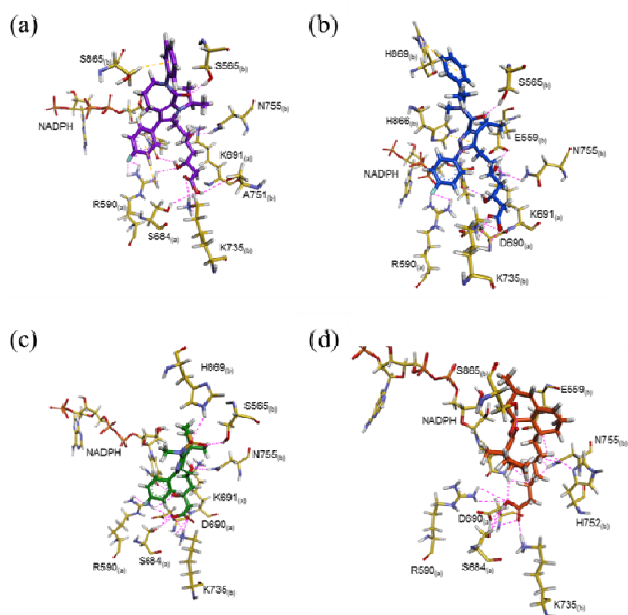


Fig. 4 Binding mode of four HMGR inhibitors at the active site. (a) INH1, (b) INH2, (c) INH3, and (d) INH4 were shown as as purple, blue, green, and orange stick model and active site residues were drawn as yellow stick model. Dash lines indicate hydrogen bond (magenta) and hydrophobic interaction (yellow), respectively

#### E. Structure-Based Pharmacophore Models

To find novel scaffolds for Anti-hypercholesterolemia drug, we generate structure-based pharmacophore models using representative structure of each system. In each case, we chosen best model having high selectivity score and diverse pharmacophoric features as final pharmacophore model of each system named as Pharm 1, Pharm 2, Pharm3, and Pharm 4, respectively. These models were subjected to validation process using data set. All pharmacophores successfully picked 12 HMGR inhibitors in data set.

#### F. Virtual Screening and Drug-Like Properties

The validated four pharmacophore models were used as 3D queries to search virtual leads for HMGR inhibitor design. From the screening, compounds mapped on pharmacophoric features of each model were selected and then filtered using drug-like properties calculation like Lipinski's rule of five and ADMET. In this process, 160, 419, 110, and 64 compounds were retrieved by Pharm 1, Pharm 2, Pharm 3, and Pharm 4. Consequently, we identified 105 compounds that commonly

present in the screening results by at least two pharmacophore models and these compounds were used for molecular docking studies.

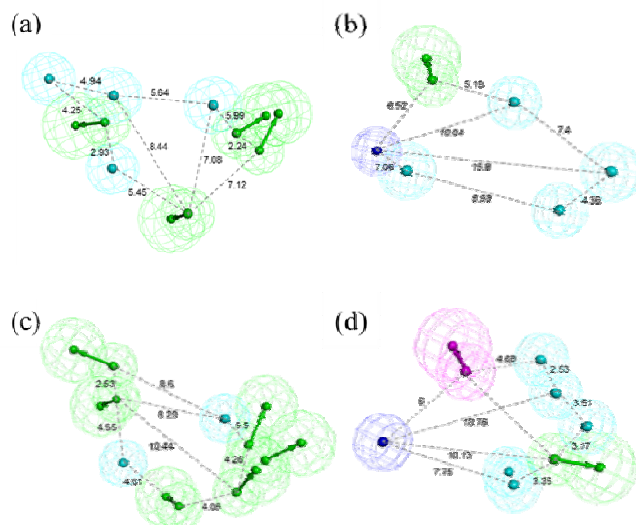


Fig. 5 Structure-based pharmacophore models of each complex. (a) Pharm 1, (b) Pharm2, (c) Pharm3, and (d) Pharm 4. HBA, HBD, HYP, and NI features were represented in green, magenta, cyan, and blue color, respectively

#### G. Selecting Final Hits using Molecular Docking

With four HMGR inhibitors, total 109 compounds were docked into active site of HMGR. Four HMGR inhibitors have GOLD fitness score of 50.74, 53.81, 52.17, and 53.05 for INH1, INH2, INH3, and INH4, respectively. Based on these fitness score and molecular interactions, we selected 32 compounds and binding free energy was calculated using these compounds. Taken together, four hit compounds were obtained and these complexes were refined by energy minimization.

#### H. Binding Mode of Final Hit Compounds

Four structures in complex with final hit compounds were obtained after energy minimization. Binding modes of final hit compounds were shown in Fig. 6. First, Hit 1 was identified by Pharm 1 and Pharm 3 and GOLD fitness score for Hit 1 was the highest value of 87.02 and binding free energy was -7.77. Hydrogen bond interactions with active site residues were found at almost oxygen atoms existent in Hit 1. The hydrogen atom of H866 was also hydrogen bonded to oxygen of carboxylic acid moiety in Hit 1 and neighboring oxygen interacted with S565 from the other monomer. The oxygen atom connecting the two phenyl rings of Hit 1 was formed hydrogen bond with R568. Second, Hit 2 scored GOLD fitness score of 78.01 and binding free energy of -6.94 was retrieved using Pharm 2 and Pharm 3. This compound also has formed numerous interactions with active site residues. Hydrogen bonds between butyramide moieties of Hit 8 matching HBA features and residues like S684, K692, S565, R568, K735, H752, N755, S852, and H866 were observed. Third, Hit 3 attained from virtual screening through Pharm 1 and Pharm 3 has GOLD fitness score of 75.76 and binding free energy of -8.01. Several active site residues formed hydrogen bonds with Hit 3. The residues R590, S684, and K692 formed hydrogen

bonding with carboxylic acid moieties of Hit 3 thiazole ring in Hit 3 has hydrogen bond interactions with K691 and N755 and neighboring NH group was hydrogen bonded to E559. The sulfonyl moiety made hydrogen bonds with C561, S865, and H866. The last hit, the GOLD fitness score and binding free energy for Hit 4 were 72.18 and -7.87, respectively. Two ether groups of Hit 4 showed hydrogen bond interactions with R590, S684, and K692, especially K692 has formed tripartite hydrogen bond. The piperidine group of Hit 4 formed bipartite hydrogen bonds with hydrogen atoms of N755 and oxygen atom close to piperidine group was also shown hydrogen bond interaction with H866. The butyramide moieties of Hit 4 made hydrogen bond interactions with S565 and S865, respectively. The binding mode analysis indicates that all final hits have favorable molecular interactions at the active site of HMGR. The novelty of final hits for the inhibition of HMGR was confirmed using SciFinder scholar [28] and PubChem structure search [29].

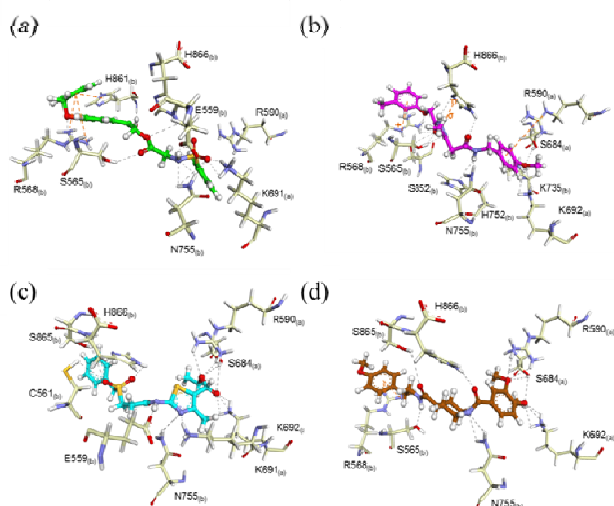


Fig. 6 Binding conformation of final hit compounds. (a) Hit 1, (b) Hit 2, (c) Hit 3, and (d) Hit 4 were represented in yellow-green, magenta, cyan, and brown stick models. Hydrogen bond and hydrophobic interactions were shown as gray and orange dash lines

#### IV. CONCLUSION

Inhibition of HMGR enzyme is considered as a way of anti-hypercholesterolemia drug development. Four compounds obtained from our study might be potential leads for developing potent inhibitor of HMGR.

#### ACKNOWLEDGMENT

This research was supported by Basic Science Research Program (2012R1A1A4A01013657), Pioneer Research Center Program (2009-0081539), and Management of Climate Change Program (2010-0029084) through the National Research Foundation of Korea (NRF) funded by the Ministry of Education, Science and Technology (MEST) of Republic of Korea. And this work was also supported by the Next-Generation BioGreen 21 Program (PJ008038) from Rural Development Administration (RDA) of Republic of Korea.

#### REFERENCES

- [1] E.S. Istvan, J. Deisenhofer, "The structure of the catalytic portion of human HMG-CoA reductase", *Biochimica et Biophysica Acta (BBA)-Molecular and Cell Biology of Lipids*, vol.1529, pp. 9-18, 2000.
- [2] L. Taberner, D.A. Bochar, V.W. Rodwell, C.V. Stauffacher, "Substrate-induced closure of the flap domain in the ternary complex structures provides insights into the mechanism of catalysis by 3-hydroxy-3-methylglutaryl-CoA reductase", *Proceedings of the National Academy of Sciences*, vol. 96, pp. 7167, 1999.
- [3] E.S. Istvan, J. Deisenhofer, "Structural mechanism for statin inhibition of HMG-CoA reductase", *Science*, vol. 292, pp. 1160-1164, 2001.
- [4] E. Boumendil, P. Tubert-Bitter, "Depression-induced absenteeism in relation to antihyperlipidemic treatment: a study using GAZEL cohort data", *Epidemiology*, pp. 322-325, 1995.
- [5] T. Phan, J. McLeod, J. Pollard, O. Peiris, A. Rohan, J. Halpern, "Peripheral neuropathy associated with simvastatin", *Journal of Neurology, Neurosurgery & Psychiatry*, vol. 58, pp.625-628, 1995.
- [6] E. Proksch, "Antilipemic drug-induced skin manifestations", *Hautarzt*, vol. 46, pp. 76, 1995.
- [7] S. John, S. Thangapandian, K.W. Lee, "Potential human cholesterol esterase inhibitor design: benefits from the molecular dynamics simulations and pharmacophore modeling studies", *J. Biomol. Struct. Dyn.*, vol. 29, pp. 921-936, 2012.
- [8] J.A. Pfefferkorn, C. Choi, Y. Song, B.K. Trivedi, S.D. Larsen, V. Askew, L. Dillon, J.C. Hanselman, Z. Lin, G. Lu, "Design and synthesis of novel, conformationally restricted HMG-CoA reductase inhibitors", *Bioorg. Med. Chem. Lett.*, vol. 17, pp. 4531-4537, 2000.
- [9] J.A. Pfefferkorn, C. Choi, S.D. Larsen, B. Auerbach, R. Hutchings, W. Park, V. Askew, L. Dillon, J.C. Hanselman, Z. Lin, "Substituted Pyrazoles as Hepatoselective HMG-CoA Reductase Inhibitors: Discovery of (3R,5R)-7-[2-(4-F luoro-phenyl)-4-isopropyl-5-(4-methyl-benzylcarbamoyl)-2H-pyrazol-3-yl]-3,5-dihydroxyheptanoic Acid (PF-3052334) as a Candidate for the Treatment of Hypercholesterolemia", *J. Med. Chem.*, vol. 51, pp. 31-45, 2007.
- [10] H.J.C. Berendsen, D. van der Spoel, R. van Drunen, "GROMACS: A message-passing parallel molecular dynamics implementation", *Comput. Phys. Commun.*, vol. 91, pp. 43-56, 1995.
- [11] D. Van Der Spoel, E. Lindahl, B. Hess, G. Groenhof, A.E. Mark, H.J.C. Berendsen, "GROMACS: fast, flexible, and free", *Journal of computational chemistry*, vol. 26, pp. 1701-1718, 2005.
- [12] V. Zoete, M.A. Cuendet, A. Grosdidier, O. Michielin, "SwissParam: A fast force field generation tool for small organic molecules", *Journal of computational chemistry*, 2011.
- [13] H. Berendsen, J. Postma, W. Van Gunsteren, J. Hermans, "Interaction models for water in relation to protein hydration" *Intermolecular forces*, vol. 331, pp. 331, 1981.
- [14] W.L. Jorgensen, J. Chandrasekhar, J.D. Madura, R.W. Impey, M.L. Klein, "Comparison of simple potential functions for simulating liquid water", *J. Chem. Phys.*, vol. 79, pp. 926, 1983.
- [15] J.P. Ryckaert, G. Ciccotti, H.J.C. Berendsen, "Numerical integration of the cartesian equations of motion of a system with constraints: molecular dynamics of n-alkanes", *Journal of Computational Physics*, vol. 23, pp. 327-341, 1977.
- [16] B. Hess, H. Bekker, H.J.C. Berendsen, J.G.E.M. Fraaije, "LINCS: a linear constraint solver for molecular simulations", *Journal of computational chemistry*, vol. 18, pp. 1463-1472, 1997.
- [17] S. Miyamoto, P.A. Kollman, "SETTLE: an analytical version of the SHAKE and RATTLE algorithm for rigid water models", *Journal of computational chemistry*, vol. 13, pp. 952-962, 1992.
- [18] T. Darden, D. York, L. Pedersen, "Particle mesh Ewald: An N · log (N) method for Ewald sums in large systems", *J. Chem. Phys.*, vol. 98, pp. 10089, 1993.
- [19] U. Essmann, L. Perera, M.L. Berkowitz, T. Darden, H. Lee, L.G. Pedersen, "A smooth particle mesh Ewald method", *J. Chem. Phys.*, vol. 103, pp. 8577, 1995.
- [20] M. Parrinello, A. Rahman, "Polymorphic transitions in single crystals: A new molecular dynamics method", *J. Appl. Phys.*, vol. 52, pp. 7182-7190, 1981.
- [21] H.J.C. Berendsen, J.P.M. Postma, W.F. Van Gunsteren, A. DiNola, J. Haak, "Molecular dynamics with coupling to an external bath", *J. Chem. Phys.*, vol. 81, pp. 3684, 1984.
- [22] C.A. Lipinski, F. Lombardo, B.W. Dominy, P.J. Feeney, "Experimental and computational approaches to estimate solubility and permeability in

- drug discovery and development settings<sup>1</sup>”, *Adv. Drug Deliv. Rev.*, vol. 46, pp. 3-26, 2001.
- [23] W.P. Walters, M.A. Murcko, “Prediction of 'drug-likeness'”, *Adv. Drug Deliv. Rev.*, vol. 54, pp. 255-271, 2002.
- [24] G. Jones, P. Willett, R.C. Glen, A.R. Leach, R. Taylor, “Development and validation of a genetic algorithm for flexible docking<sup>1</sup>”, *J. Mol. Biol.* 267, vol. 267, pp. 727-748, 1997.
- [25] M.L. Verdonk, J.C. Cole, M.J. Hartshorn, C.W. Murray, R.D. Taylor, “Improved protein–ligand docking using GOLD”, *Proteins: Structure, Function, and Bioinformatics.*, vol. 52, pp. 609-623, 2003.
- [26] G.M. Morris, D.S. Goodsell, R.S. Halliday, R. Huey, W.E. Hart, R.K. Belew, A.J. Olson, “Automated docking using a Lamarckian genetic algorithm and an empirical binding free energy function”, *Journal of computational chemistry.*, vol. 19, pp. 1639-1662, 1998.
- [27] G.M. Morris, R. Huey, W. Lindstrom, M.F. Sanner, R.K. Belew, D.S. Goodsell, A.J. Olson, “AutoDock4 and AutoDockTools4: Automated docking with selective receptor flexibility”, *Journal of computational chemistry.*, vol. 30, pp. 2785-2791, 2009..
- [28] A.B. Wagner, “SciFinder Scholar 2006: an empirical analysis of research topic query processing”, *Journal of chemical information and modeling.*, vol. 46, pp. 767-774, 2006.
- [29] Y. Wang, E. Bolton, S. Dracheva, K. Karapetyan, B.A. Shoemaker, T.O. Suzek, J. Wang, J. Xiao, J. Zhang, S.H. Bryant, “An overview of the PubChem BioAssay resource”, *Nucleic Acids Res.*, vol. 38, pp. D255-D266, 2010.